



ALMA MATER STUDIORUM  
UNIVERSITÀ DI BOLOGNA

ARCHIVIO ISTITUZIONALE  
DELLA RICERCA

## Alma Mater Studiorum Università di Bologna Archivio istituzionale della ricerca

Parabrachial complex links pain transmission to descending pain modulation

This is the final peer-reviewed author's accepted manuscript (postprint) of the following publication:

*Published Version:*

Parabrachial complex links pain transmission to descending pain modulation / Roeder, Zachary; Chen, Qiliang; Davis, Sophia; Carlson, Jonathan D.; Tupone, Domenico; Heinricher, Mary M. - In: PAIN. - ISSN 0304-3959. - ELETTRONICO. - 157:12(2016), pp. 2697-2708. [10.1097/j.pain.0000000000000688]

*Availability:*

This version is available at: <https://hdl.handle.net/11585/585822> since: 2017-05-11

*Published:*

DOI: <http://doi.org/10.1097/j.pain.0000000000000688>

*Terms of use:*

Some rights reserved. The terms and conditions for the reuse of this version of the manuscript are specified in the publishing policy. For all terms of use and more information see the publisher's website.

This item was downloaded from IRIS Università di Bologna (<https://cris.unibo.it/>).  
When citing, please refer to the published version.

(Article begins on next page)



Published in final edited form as:

*Pain*. 2016 December ; 157(12): 2697–2708. doi:10.1097/j.pain.0000000000000688.

## The parabrachial complex links pain transmission to descending pain modulation

Zachary Roeder<sup>1,†</sup>, QiLiang Chen<sup>1,†</sup>, Sophia Davis<sup>1</sup>, Jonathan D. Carlson<sup>1</sup>, Domenico Tupone<sup>1</sup>, and Mary M. Heinricher<sup>1,2</sup>

<sup>1</sup>Department of Neurological Surgery, Oregon Health & Science University, Portland, OR 97239

<sup>2</sup>Department of Behavioral Neuroscience, Oregon Health & Science University, Portland, OR 97239

### Abstract

The rostral ventromedial medulla (RVM) has a well-documented role in pain modulation, and exerts anti-nociceptive and pro-nociceptive influences mediated by two distinct classes of neurons, OFF-cells and ON-cells. OFF-cells are defined by a sudden pause in firing in response to nociceptive inputs, whereas ON-cells are characterized by a “burst” of activity. Although these reflex-related changes in ON- and OFF-cell firing are critical to their pain-modulating function, the pathways mediating these responses have not been identified. The present experiments were designed to test the hypothesis that nociceptive input to the RVM is relayed through the parabrachial complex (PB). In electrophysiological studies, ON- and OFF-cells were recorded in the RVM of lightly anesthetized male rats before and after an infusion of lidocaine or muscimol into PB. The ON-cell burst and OFF-cell pause evoked by noxious heat or mechanical probing were substantially attenuated by inactivation of the lateral, but not medial, parabrachial area. Retrograde tracing studies showed that neurons projecting to the RVM were scattered throughout PB. Few of these neurons expressed calcitonin gene-related peptide (CGRP), suggesting that the RVM projection from PB is distinct from that to the amygdala.

These data show that a substantial component of “bottom-up” nociceptive drive to RVM pain-modulating neurons is relayed through the parabrachial complex. While the parabrachial complex is well-known as an important relay for ascending nociceptive information, its functional connection with the RVM allows the spinoparabrachial pathway to access descending control systems as part of a recurrent circuit.

### 1. Introduction

An important factor in both acute and chronic pain is an intrinsic pain-modulating system that regulates nociceptive processing via descending projections from the brainstem to the dorsal horn. This system contributes to abnormal pain in animal models; in patients,

---

Address correspondence to: Mary M. Heinricher, Ph.D., Department of Neurological Surgery, Oregon Health & Science University, Portland, OR 97239, 503-494-1135, heinricm@ohsu.edu.

<sup>†</sup>These authors contributed equally to this work

The authors report no conflict of interest.

impaired descending control has been documented in many chronic pain syndromes.<sup>15,20,31,35,48,59,60,69,72,77</sup> The output of this modulating system, via the rostral ventromedial medulla (RVM), can facilitate or suppress nociception via two physiologically-defined cell classes, “ON-cells” and “OFF-cells,” that respectively facilitate and inhibit dorsal horn nociceptive transmission.<sup>31,32,35</sup> However, these modulatory neurons also *receive* noxious input: ON-cells are activated by noxious stimulation, giving a “burst” of activity, whilst OFF-cell firing is suppressed, producing a “pause” in any ongoing activity. This acute activation of pain-facilitating ON-cells and suppression of pain-inhibiting OFF-cells can function as a positive feedback loop, promoting responses to subsequent afferent inputs.<sup>38,42</sup> Pain transmission and modulating systems thus constitute a recurrent circuit, with noxious stimulation as the primary “bottom-up” influence on pain-modulating outputs. Surprisingly, the pathway through which noxious inputs drive changes in RVM activity has not been defined. Not knowing how pain transmission is linked to pain modulation has severely limited our ability to define the function and plasticity of the RVM at the level of the synapse, cell membrane, and circuit.

One candidate with the potential to relay noxious information to the RVM is the parabrachial complex (PB). The PB comprises a functionally and anatomically diverse region involved in a range of homeostatic functions.<sup>4,24,25,43,55</sup> It is a major supraspinal target of nociceptive transmission neurons with cell bodies in the contralateral superficial dorsal horn (with sparse ipsilateral input). It also receives projections from deep dorsal horn.<sup>6,8,22,58</sup> Nociceptive neurons have been identified in the PB, primarily in lateral PB (IPB) and the Kölliker-Fuse nucleus (KF).<sup>5,7,9,37</sup> There is evidence that spinal neurokinin-1 (NK1)-positive neurons, presumed to relay through PB, engage both descending inhibition and descending facilitation.<sup>47,68,74</sup>

A direct, but relatively sparse projection from the PB to the RVM region has been identified anatomically.<sup>3,36,75</sup> In addition, PB projects directly to the central nucleus of the amygdala and through a thalamic relay to the insula, implicating the PB in emotional and autonomic aspects of pain.<sup>9,25,40,78</sup> It also projects to the midbrain periaqueductal gray.<sup>26</sup> Each of these parabrachial targets has outputs that converge, directly or indirectly, at the RVM.<sup>41,51,52,65</sup> Despite these wide-reaching anatomical links, the functional influence of PB on RVM pain-modulating neurons has not been investigated.

The present experiments were designed to test the hypothesis that nociceptive input to pain-modulating neurons of the RVM is relayed through the PB. We also used immunohistochemical methods to determine whether the projection from PB to RVM includes CGRP neurons, since CGRP-expressing neurons comprise a significant proportion of the nociception-related projection from PB to the amygdala.<sup>18,27,66</sup> We found that blocking the lateral PB complex, but not the medial PB are, significantly attenuated nociceptive responses of RVM pain-modulating neurons, indicating that a substantial component of pain-related drive to RVM pain-modulating neurons is relayed through the lateral PB.

## 2. Materials and Methods

All experimental procedures were approved by the Institutional Animal Care and Use Committee at Oregon Health & Science University and followed the guidelines of the Committee for Research and Ethical Issues of the International Association for the Study of Pain.

### 2.1. Electrophysiological experiments

**2.1.1. Animal preparation**—Male Sprague-Dawley rats were purchased from Charles River (240–340 g) and acclimated for at least one week in the vivarium with a 12-h light/dark cycle and food and water available *ad libitum*. Experiments were performed during the light phase.

On the day of the experiment, animals were deeply anesthetized (isoflurane) and a catheter inserted in the external jugular vein for subsequent infusion of the short-acting barbiturate methohexital. They were then transferred to a stereotactic frame. Small craniotomies were made to gain access to the RVM and PB, and the meninges were opened. Heart rate was monitored using EKG, and respiratory rate using a ventilation pressure transducer.<sup>16</sup> Body temperature was monitored and maintained at 36–37 °C with a heating pad. When preparatory surgeries were complete, rats were placed on a continuous methohexital infusion. The anesthetic plane was set at a depth that allowed a stable heat-evoked hindpaw withdrawal reflex, while preventing spontaneous movement. Animals were stabilized for at least 45 minutes at an anesthetic flow rate before beginning data collection.

**2.1.2. Microinjections**—Drugs were delivered to the PB using a glass microinjector (70 µm outer diameter) attached to a 1 µl Hamilton syringe using PE50 tubing. Lidocaine (4%), the GABA<sub>A</sub> receptor agonist muscimol (8 pmol), or artificial cerebrospinal fluid (aCSF, comprised of NaCl 128 mM, KCl 2.6 mM, CaCl<sub>2</sub> dihydrate 1.3 mM, MgCl<sub>2</sub> hexhydrate 0.9 mM, NaHCO<sub>3</sub> 20 mM, Na<sub>2</sub>HPO<sub>4</sub> 1.3 mM, with pH of 7.4) was injected in 200 nl over a period of 3 to 4 min. Fluorescent beads (FluoSpheres, Invitrogen, Eugene, OR) were included in the drug solutions in a 1:100 concentration to verify the injection site, and injectors were rinsed before being lowered into the brain. Injections were generally made into the right lateral PB (contralateral to stimulation of the left hindpaw), but in some experiments, injections were made bilaterally. Stereotactic coordinates (relative to interaural zero, head level) were as follows: lateral PB (AP –1.2 mm with the injector directed caudally at 14°, ML ± 2.3 mm, DV +3; right medial parabrachial area (mPB) (off-target placement controls; AP –1.2 mm with the injector directed caudally at 14°, ML –1.4 mm, DV +3).

**2.1.3. Extracellular recording**—Extracellular single-unit recordings were made with stainless-steel microelectrodes (Microprobes, Gaithersburg, MD) with gold- and platinum-plated tips. Signals were amplified (10k) and bandpass filtered (400 Hz to 15 kHz) before analog-to-digital conversion at 32k samples/s.

An RVM neuron was isolated and classified as an ON-, OFF-, or NEUTRAL-cell using methods described previously.<sup>1,15</sup> Both ON- and OFF-cells have whole body receptive

fields, but inverse responses during nocifensive behaviors. That is, ON-cells exhibit a burst of action potentials beginning immediately before a nocifensive withdrawal or continue firing if already active. OFF-cells cease firing (if active), or remain silent (if inactive). NEUTRAL-cells show no response associated with nocifensive reflexes, as described previously.<sup>1,15</sup> To further confirm cell classification, a 10 s noxious pinch was delivered to the hindpaw using a toothed forceps: ON-cells fire and OFF-cells cease firing throughout the stimulus. Activity of only one neuron was recorded in a typical experiment, but that of more than one neurons was recorded simultaneously in seven cases (of 94 total).

**2.1.4. Experimental protocol**—An ON-, OFF-, or NEUTRAL-cell was isolated. Lidocaine or muscimol was used to block PB and effects on spontaneous firing and changes in cell activity associated with nociceptive withdrawal reflexes were then determined.

Both noxious heat and von Frey fiber stimulation of the hindpaw were used. For heat-evoked withdrawal, the left hindpaw was placed on a platform overlying a feedback-controlled halogen bulb, with trials at approximately 5 min intervals. The paw surface temperature was increased at a rate of 1.2 °C/s from 35 °C to a maximum of 53 °C. The withdrawal temperature and latency were determined using a transducer attached to the paw. Withdrawals evoked by mechanical stimuli (von Frey filaments) were also tested in a separate set of experiments. Filaments (26, 60, and 100 g) were applied, in ascending order, to the interdigital webbing of the plantar surface of the left hindpaw for 8 s, with three trials of each force. A minimum of two testing sites was used in rotation. Individual trials were initiated at intervals of at least 30 s, with longer interstimulus intervals (up to 2 min) used when necessary to capture a period when the cell under study was inactive (ON-cell) or active (OFF-cell) so that a “burst” or “pause” could be quantified. Withdrawals were recorded as calf muscle electromyography (EMG), with the first positive inflection of the rectified EMG used as the onset of the response. If there was no withdrawal within the stimulus period (15 s for heat, 8 s for mechanical stimuli), this cut-off latency (i.e., 15 or 8 s) was assigned for assessment of response latencies.

For heat stimulation, lidocaine, muscimol, or aCSF was infused into the right lateral PB complex (contralateral to the stimulated paw), right medial parabrachial area, or both the left and right lateral PB following a baseline period with four trials. Additional trials were performed after the infusion was complete, for a total time of up to one hour. Trials were initiated at approximately 5 min intervals throughout, as noted above. For mechanical stimulation, lidocaine was infused into the right lateral PB nucleus (contralateral to the stimulated paw) following a baseline consisting two sets of the von Frey stimulus series. Two additional von Frey stimulus series were then delivered over the 10 to 15 min period after completing the microinjection. As noted above, individual trials were initiated at intervals of at least 30 s, with longer interstimulus intervals (up to 2 min) used when needed in an attempt capture a period when the cell under study was inactive (ON-cell) or active (OFF-cell) so that a “burst” or “pause” could be quantified. If the ON-cell remained active or OFF-cell silent beyond those limits, no “burst” or “pause” data were obtained for that trial.

**2.1.5. Data analysis**—The extracellular recording signal, EMG, EKG, and respiratory transducer output were digitized and collected using Spike 2 software (Cambridge

Electronics Design Ltd, Cambridge, UK). Each waveform was sorted using Spike2 template matching and cluster analysis, and verified on an individual spike basis.

A number of cell parameters, defined as previously described,<sup>1,11,50</sup> were used to characterize reflex-related changes in RVM cell activity. In experiments testing heat-evoked withdrawals, we analyzed the number of spikes per ON-cell burst, the latency from burst onset to hindpaw withdrawal, and the peak firing rate during the burst. For OFF-cells, we analyzed the duration of the OFF-cell pause and the latency from the pause to hindpaw withdrawal. In experiments testing mechanically-evoked withdrawals, we analyzed spontaneous activity (firing rate in the 30 s period before stimulus sets), number of spikes per ON-cell burst, and the duration of the OFF-cell pause.

Data were compared between average baseline and post-drug times appropriate for each agent. For lidocaine, the testing protocol was completed within 15 min of the injection. For muscimol, which has a longer duration of action than lidocaine, the mean of heat trials at 10, 15 and 20 min post-injection was used as the post-drug response.

Latencies were analyzed using a paired *t*-test or Wilcoxon's signed ranks test to compare post-block responses to baseline (the latter when the distribution of responses was truncated because some responses were at the cut-off value). Because cell parameters for RVM neurons are typically highly skewed, some were analyzed using paired *t*-test of log-transformed data, again comparing post-block responses to baseline. For all tests,  $p < 0.05$  was considered significant. Data are reported as mean and SEM or, for log-transformed data, geometric mean with 95% confidence limits.

**2.1.6. Injection and recording sites**—At the completion of the recording, an electrolytic lesion was made in the RVM to localize the recording site. Rats were overdosed with methohexital and transcardially perfused. The brains were removed and sectioned on a Leica CM3050 S cryostat (60  $\mu$ m sections). The RVM lesion and fluorescent beads marking the injection site in the PB region were photographed with an Optronics Microfire camera attached to an Olympus BX51 microscope. If beads or lesion were not found, the data were not analyzed further. Injection sites were plotted on hand-drawn sections in Adobe Illustrator using landmarks defined by Paxinos and Watson.<sup>57</sup> For “on-target” injections, if injection sites were not located within the lateral parabrachial complex, the data were not analyzed further. The RVM was defined as the nucleus raphe magnus and adjacent reticular formation medial to the lateral boundary of the pyramids at the level of the facial nucleus.

## 2.2. Anatomical study of projections from PB to RVM and overlap with CGRP expression

**2.2.1. Animal preparation**—Two adult male Wistar rats, anesthetized with 3% isoflurane in 100% O<sub>2</sub>, were injected with fluorogold (FG, 4%, 30nl, Fluorochrome, LLC) into RVM (stereotactic coordinates: AP -3.0 mm, ML 0 mm, DV -9.2 mm relative to lambda with incisor bar at -4 mm). Rats were treated with antibiotic (40,000 units/kg penicillin G, s.c.), analgesic (0.05 mg/kg buprenorphine, s.c.) and saline (3 ml, s.c.). After 7 days, the rats were deeply anesthetized with pentobarbital (80 mg/kg, i.p.) and transcardially perfused with 200 ml isotonic saline followed by 200 ml paraformaldehyde (4% in PBS). The brains were post-fixed in 4% paraformaldehyde for 1 h and equilibrated overnight in PBS with 30% sucrose

and 0.01% sodium azide. Serial coronal sections (30  $\mu\text{m}$ ) were cut with a freezing-stage microtome, collected sequentially in 6 sets and stored in PBS with 0.01% sodium azide at 4  $^{\circ}\text{C}$ .

**2.2.2. Immunohistochemical procedures**—Sections containing PB were pre-incubated in an antibody dilution solution (ADS: 500 ml PBS, 0.3% Triton-X 100, 1.25 g carrageenan, 100 mg  $\text{NaN}_3$ , 5 ml normal donkey serum) for 3 h and incubated overnight at room temperature with the primary antibodies for CGRP (1:2000, Mouse-anti-CGRP, Ab81887, Abcam) and FG (1:70,000, Rabbit-anti-Fluoro-Gold, 52–9600, Fluorochrome, LLC). After two washes in PBS containing 0.3% Triton-X 100 (TPBS, 20mM), the tissue was incubated for 1 h in ADS containing the secondary antibody for CGRP (1:500, Alexa Fluor594-donkey-anti-Mouse, Invitrogen). After two washes in TPBS, the tissue was incubated for 1 h in ADS containing the secondary antibody for FG (1:500, AlexaFluor488-donkey-anti-Rabbit, Invitrogen). After fluorescent labeling, the tissue was washed in PBS and mounted onto coated slides, air dried and coverslipped with anti-fade mounting medium (Pro-Long Gold, Invitrogen).

**2.2.3. Tissue analysis**—The neuroanatomical designations of the injection sites in RVM and those of FG- and CGRP-labeled neurons in the PB are based on the stereotaxic rat brain atlas of Paxinos and Watson.<sup>57</sup> Photomicrographs of brain sections and labeled neurons were taken with a camera attached to an Olympus BX51 fluorescence microscope. The photomicrographs were assembled into a plate using Adobe Photoshop to adjust contrast and brightness without altering the original colors.

### 3. Results

#### 3.1. Effect of blocking lateral PB on ON- and OFF-cell firing and withdrawal evoked by noxious heat and von Frey hindpaw stimulation

Activity of RVM ON-, OFF-, and NEUTRAL-cells was recorded before and during blockade of the contralateral lateral PB complex. We successfully completed the entire protocol for a total of 39 ON-cells, 40 OFF-cells, and 7 NEUTRAL-cells in 79 animals before and after block of the lateral PB. We also recorded 8 ON-cells and 7 OFF-cells before and after block of the medial PB area (15 animals). PB injection sites are plotted in Fig 1.

Blocking the lateral PB substantially attenuated the ON-cell burst and OFF-cell pause evoked by either thermal or mechanical noxious stimulation. Fig. 2 shows representative examples of an OFF-cell and ON-cell response during heat-evoked withdrawal before and after lateral PB block. The duration of the OFF-cell pause was substantially reduced, as was the magnitude of the ON-cell burst.

Group effects are summarized in Fig. 3 for thermally evoked responses. As shown in Fig. 3A, blocking the lateral PB contralateral to a noxious heat-evoked paw withdrawal using either lidocaine or muscimol significantly attenuated the associated ON-cell burst (lidocaine:  $t_9 = 2.48$ ,  $p = 0.035$ ,  $n = 11$  with one cell active at stimulus onset, precluding quantification of the burst; muscimol:  $t_8 = 2.76$ ,  $p = 0.025$ ,  $n = 10$ , with one cell active). Infusion of aCSF into lateral PB had no effect on the ON-cell response ( $t_4 = 0.25$ ,  $p = 0.81$ ,  $n = 10$ , with five

cells active at stimulus onset). The OFF-cell pause was also significantly reduced during block of lateral PB using either lidocaine or muscimol (Fig. 3B, lidocaine:  $t_{10} = 2.52$ ,  $p = 0.03$ ,  $n = 11$ ; muscimol:  $t_7 = 3.16$ ,  $p = 0.016$ ,  $n = 8$ ). Again, vehicle infusion was without effect (aCSF:  $t_6 = 1.37$ ,  $p = 0.22$ ,  $n = 8$  with one cell silent at stimulus onset, precluding quantification of pause duration). The fact that both lidocaine and muscimol were effective suggests that the effect of the block was on lateral PB neurons, and not simply fibers of passage.

As figures 2 and 3 illustrate, the RVM response during heat-evoked withdrawal was not *eliminated* following PB block. For ON-cells, although the evoked response was reduced substantially, it was not eliminated completely (i.e., to 0 spikes associated with withdrawal). Moreover, although the OFF-cell pause was substantially reduced with lateral PB block, it remained significantly longer than the mean interspike interval in the 5 s period immediately prior to onset of the noxious stimulus. Thus, for example, although the reflex-related pause was reduced from 6.75 s [95%CI: 2.69, 16.75] in baseline to 2.2 s [95% CI: 1.21, 4.01] during muscimol block of PB, the pause remained significantly longer than the interspike interval immediately prior to heat onset for those trials (0.19 s [95% CI: 0.08, 0.43]  $t_7 = 6.9$ ,  $p = 0.0002$ ,  $t$ -test for correlated means,  $n = 8$ ). This confirms that the OFF-cell pause was not *entirely* eliminated with lateral PB block.

Similar effects of blocking lateral PB were seen when ON- and OFF-cell responses associated with mechanically evoked withdrawals were examined. Fig. 4 shows representative examples of an OFF-cell and ON-cell response during withdrawal evoked by von Frey probes before and after lateral PB block. The duration of the OFF-cell pause was substantially reduced. The ON-cell burst was eliminated in this case. These effects are quantified in Figure 5, which shows group data for ON- and OFF-cell responses during withdrawal evoked by 26, 60, or 100 g von Frey filaments in baseline and during block of the lateral PB contralateral to the stimulus using lidocaine. Both the ON-cell burst (Fig. 5A) and OFF-cell pause (Fig. 5B) were significantly attenuated, but again generally not completely eliminated, during lateral PB block.

In addition to the significant reduction in response magnitude, the *latency* of the residual response during peripheral stimulation was increased. Thus, both the pause and burst associated with heat-evoked withdrawal occurred at a longer latency during lidocaine block of PB (Fig. 6A). Vehicle (aCSF) injection had no effect on the latency of either the pause ( $t_6 = 1.21$ ,  $p = 0.34$ ,  $n = 8$  with one silent cell) or burst ( $t_7 = 0.88$ ,  $p = 0.40$ ,  $n = 10$  with two active cells). Responses during intense mechanical stimuli (60 and 100 g) also occurred at a longer latency (Fig. 6B and C).

The relationship between the neuronal response and the behavioral withdrawal was not altered, with no overall change in the latency from the onset of the residual neuronal response to withdrawal during lateral PB block. For example, the latency from withdrawal-related pause to the withdrawal itself was  $0.70 \pm 0.12$  s in baseline, and  $1.22 \pm 0.70$  s during block ( $t_{10} = 0.71$ ,  $p = 0.49$ ,  $n = 11$ ). The latency from the withdrawal-related burst to the withdrawal itself was  $0.77 \pm 0.20$  s in baseline, and  $2.15 \pm 0.89$  s during block ( $t_9 = 1.69$ ,  $p = 0.12$ ,  $n = 11$  with one cell showing no burst during block).. Therefore, given the increase in



neuronal response latency during inactivation of lateral PB, it should not be surprising that behavioral response latency was also increased. Fig. 7A shows that latencies of heat-evoked responses were increased during lidocaine block of PB, but not following injection of aCSF. For mechanical stimuli (Fig. 7B), the change in latency of the behavioral response was significant only in the noxious range (60 and 100 g), which parallels the change in neuronal response latency described above (Fig. 6). The lack of change in both neuronal and behavioral responses with the 26 g stimulus is probably related to the fact that the proportion of cut-off values was relatively high with this filament. (Even in baseline, half of the 22 animals tested showed no response within the 8 s cut-off time at this stimulus intensity, Fig. 7B).

In addition to the attenuation of withdrawal-related changes in firing, PB block altered the spontaneous discharges of both ON- and OFF-cells. As shown in Fig. 8, lidocaine block of lateral PB resulted in a significant increase in the spontaneous firing of OFF-cells and a decrease in the ongoing firing of ON-cells. NEUTRAL-cell firing was unaffected by parabrachial blockade.

### 3.2. Bilateral lateral PB block does not completely eliminate ON- and OFF-cell reflex-related activity

As described above, the ON-cell burst and OFF-cell pause were largely attenuated by unilateral blockade of the lateral PB contralateral to the noxious stimulus, but they were rarely fully abolished. To determine whether the burst and pause could be eliminated *completely* with block of lateral PB bilaterally, we recorded from 4 ON-cells and 5 OFF-cells before and after bilateral lidocaine or muscimol injections (ipsilateral and contralateral to the noxious stimulus). In neither case was the response entirely abolished with the ON-cells showing at least one reflex-related spike in all cases, and the OFF-cells similarly exhibiting a pause that was at least three times the mean interspike interval in the 5-s period immediately before the stimulus onset. Thus, the average number of evoked spikes in the ON-cell burst was 16.8 [range: 3.8 – 50.0] in baseline and 6.3 [range: 0.67 – 16] during bilateral PB block. The duration of the OFF-cell pause was reduced from 55.4 s [range: 11.0 to 136.1] in baseline to 13.9 s [range: 3.4 – 34.1] during PB block.

### 3.3. Off-target placement control injections

Anatomical studies show a direct projection from the dorsal horn to the lateral PB, and Fos expression evoked by noxious hindpaw stimulation is mainly restricted to lateral PB.<sup>37</sup> The medial PB area therefore provided a reasonable off-target placement control site. We tested the effect of blocking the medial PB and adjacent tegmentum on the responses of ON-cells and OFF-cells during heat-evoked withdrawal. Neither the ON-cell burst nor the OFF-cell pause were significantly reduced following infusion of muscimol in medial controls sites (Fig. 9). Paw withdrawal latency was also unaffected (baseline:  $2.6 \pm 0.4$ s, block:  $2.7 \pm 0.5$ s;  $t_{14} = 0.29$ ,  $p = 0.77$ ,  $n = 15$ ).

### 3.4. CGRP-expressing neurons in PB do not project to RVM

The neuropeptide CGRP has been proposed to have important roles in a number of pain syndromes. CGRP-immunoreactive (ir) neurons in PB are thought to contribute to the

affective component of a nociceptive experience through a projection to the central nucleus of amygdala.<sup>18,66</sup> However, it is unclear whether CGRP-positive neurons also project directly to the RVM. To address this question, we injected the retrograde tracer FG in RVM (Fig. 10). The tracer injection extended about 1 mm rostral and caudal from the focus of the injection, covering a large portion of the raphe magnus and dorsal parapyramidal area. FG-ir neurons in PB demonstrate projections to RVM arising from the Kölliker-Fuse nucleus, the lateral PB, including the dorsal, crescent, and central lateral nuclei, and more sparsely, from medial PB (Fig. 10).

Immunostaining for CGRP revealed a population of neurons extending from 0.24 anterior to 0.36 posterior to the interaural line (Fig. 10), confirming previous observations.<sup>46,66,78</sup> However, only one CGRP-ir neuron in PB was found to be double-labeled for FG (Fig. 10). Indeed, the population of neurons projecting to RVM seemed to be segregated from the CGRP-ir neurons in PB. The dense plexus of CGRP-ir fibers in PB prevented an accurate analysis of the number of CGRP-ir neurons in the region. Nevertheless, the distribution of FG-ir neurons did not overlap with that of CGRP in PB, as shown in the example in Fig. 10.

#### 4. Discussion

The RVM is the output node of an intrinsic brain pain-modulating circuit that can facilitate or inhibit pain depending on stimulus history (e.g., persistent inflammation) as well as “top-down” cognitive and emotional factors.<sup>31,32,35</sup> The interactions between the *inputs* to the RVM and its *output* form a recurrent positive and negative feedback network that are important for acute and persistent pathological pain. Analysis of the *output* of the RVM using selective pharmacological manipulation has shown that the facilitatory and inhibitory outputs of the RVM are represented by ON-cells and OFF-cells.<sup>31,32,35</sup>

The *inputs* to the RVM are less well understood. “Top-down” inputs, e.g., from the amygdala, periaqueductal gray, and hypothalamus, have been implicated in modulation of pain during stress, fear, and immune activation,<sup>31,34,35,49,52</sup> although the relevant circuitry is just beginning to be elucidated. The primary “bottom-up” input to RVM is nociceptive sensory information: pain-facilitating ON-cells are activated by noxious stimuli, whereas the pain-inhibiting OFF-cells cease firing. These changes in firing are abrupt, and time-locked to the behavioral withdrawal from the stimulus,<sup>23</sup> forming a positive feedback loop. Despite the well-known fact that RVM ON- and OFF-cells respond to noxious somatic stimuli, the specific pathways through which nociception-related information reaches RVM pain-modulating neurons in acute and chronic pain states had not previously been identified.

The present experiments provide strong evidence that a significant share of the acute nociceptive input to ON- and OFF-cells is relayed through PB, specifically lateral PB. Infusion of lidocaine into the lateral PB in normal animals substantially attenuated the ON-cell burst and OFF-cell pause evoked by either thermal or mechanical noxious stimulation contralateral to the PB injection site. Similar attenuation of the burst and pause with muscimol indicated that the effect of lidocaine was not due to inactivation of fibers of passage, e.g., to nucleus cuneiformis, a known input to RVM.<sup>2,79</sup> The reduction in the nociceptive responses of RVM ON- and OFF-cells was unlikely to be due to spread of

lidocaine or muscimol to adjacent structures, since inactivation of medially adjacent control sites in the medial PB area did not significantly attenuate either the burst or pause. These data therefore show that the lateral PB is a major relay for nociceptive inputs triggering ON- and OFF-cell responses to acute noxious stimulation. Inactivation of lateral PB also led to significant changes in the spontaneous firing of RVM ON- and OFF-cells, with an increase in OFF-cell discharge and a decrease in ON-cell discharge. This change implies that information relayed through lateral PB also contributes to the ongoing “tone” of RVM ON- and OFF-cell output, a conclusion consistent with the fact that blocking ascending transmission from the lumbar spinal cord also alters spontaneous firing of these neurons.<sup>30</sup>

The firing of RVM NEUTRAL-cells was unaffected by PB block, confirming the distinct properties of these neurons as a separate RVM cell class. However, the sample of NEUTRAL-cells here was relatively small, and we not record from raphe pallidus, a subregion of the RVM and known target of PB efferents, which has a well-documented role in thermoregulation.<sup>54</sup>

### **Parabrachial complex as a major relay for supraspinal nociceptive transmission**

PB comprises a functionally and anatomically diverse region involved in a wide range of homeostatic functions.<sup>4,24,25,43,55</sup> PB also has an important role in receiving, processing, and relaying nociceptive signals.<sup>26</sup> It is a major supraspinal target of nociceptive transmission neurons with cell bodies in the contralateral superficial dorsal horn (with sparse ipsilateral input). It also receives projections from deep dorsal horn.<sup>6,8,22,58</sup> Nociceptive neurons have been identified predominantly in the lateral PB.<sup>5,7,9,37</sup> Functionally, there is evidence that spinal NK1-positive neurons, considered to constitute the primary nociceptive input to PB, leads to engagement of both descending inhibition and facilitation.<sup>47,68</sup> However, whether the PB *itself* engages RVM pain-modulating neurons had not been tested. The present study provides direct evidence that RVM pain-modulating neurons receive nociceptive input relayed through lateral PB, which could subsequently modulate nociceptive transmission and nocifensive behaviors.

The present experiments do not define the circuitry linking PB to the RVM. Although we confirmed a direct anatomical connection from the PB to the RVM,<sup>3,36,75</sup> we cannot conclude that this projection conveys nociceptive information to RVM ON- and OFF-cells, since although RVM-projecting neurons are distributed in both medial and lateral PB, only inactivation of lateral PB interfered with nociceptive responses in the RVM. Moreover, these projections could potentially contribute to one of the other roles shared by PB and RVM (e.g., thermoregulation, cardiovascular regulation<sup>12,13,19,39,53,55,63,64</sup>). Further, there are a number of indirect connections that could mediate the PB input to RVM. Among the parabrachial targets that have outputs converging directly or indirectly at the RVM are the central nucleus of the amygdala, midbrain periaqueductal gray, and insula (through a thalamic relay).<sup>9,25,40,41,51,52,65,78</sup> In either case, our finding that RVM-projecting neurons in the PB are scattered across nuclei of the PB complex and do not generally express CGRP suggests that RVM-projecting neurons in PB are distinct from the CGRP-containing population that constitutes a substantial proportion of the PB projection to the central

nucleus of the amygdala.<sup>18,28,66</sup> Additional studies will be needed to isolate direct and indirect influences on the RVM from PB, and to define underlying synaptic mechanisms.

Although the reduction in both the ON-cell burst and OFF-cell pause during PB block was substantial, it was not complete. This could be due to a less than total elimination of lateral PB activity with either lidocaine or muscimol.<sup>17</sup> In addition, the parabrachial complex is a large elongated structure, and RVM-projecting neurons are distributed along the entire rostro-caudal axis. The blocking agents are unlikely to have spread throughout the entire complex. However, using a larger volume to influence the entire lateral PB would have unavoidably suppressed activity in surrounding structures. Another possibility is that nociceptive information is conveyed through PB ipsilateral to the noxious stimulus.<sup>5</sup> However, even *bilateral* lateral PB block was not sufficient to eliminate the burst and pause completely. This raises the possibility that additional pathways, such as a direct input from dorsal horn,<sup>67</sup> or other relays, such as the periaqueductal gray, also carry nociceptive information to the RVM.

### Functional role of the PB relay to RVM pain-modulating neurons

The ongoing “tone” of ON- and OFF-cell firing shifted during PB block, with increased ON-cell firing and decreased OFF-cell firing, and the ON-cell burst and OFF-cell pause were delayed, not eliminated. The withdrawal reflex latency increased in parallel with the delay in the burst and pause. This modest increase in withdrawal latency is consistent with the known subtle influence of ongoing RVM ON- and OFF-cell activity on withdrawal threshold under basal conditions,<sup>29,33</sup> and with the fact that elimination of the majority of dorsal horn neurons projecting to PB using a toxin selective for neurons expressing the NK1 receptor similarly has no or limited effects on nociceptive behaviors under basal conditions.<sup>44,56,62,68</sup>

The PB input to RVM may nevertheless play an important role in hyperalgesia and persistent pain, in which both structures have been implicated. Hyperalgesia and sensitization of dorsal horn neurons in models of injury, inflammation, and neuropathy either fails to develop or is significantly attenuated following elimination of NK1-expressing neurons, the major nociceptive input to the parabrachial complex.<sup>44,56,62,68</sup> Similarly, interfering with ON-cell activation in acute inflammatory states attenuates behavioral hypersensitivity.<sup>15,45,76</sup> Moreover, there is abundant indirect evidence that ON-cells contribute to hyperalgesia in neuropathy, opioid-induced hyperalgesia, and other persistent pain states.<sup>10,14,21,59,62,70,71,73</sup> A better understanding of the interactions between the PB and RVM in conditions of injury and inflammation should therefore provide critical insights into the plasticity of pain-modulation in persistent pain.<sup>11,15,20,61</sup>

### Conclusion

Despite over 30 years of research on descending control, the pathway(s) through which noxious inputs drive changes in brainstem pain-modulating activity had not previously been defined. The present experiments have identified PB as a major relay through which noxious stimulation, the primary “bottom-up” influence on pain-modulating circuits, reaches the RVM to influence activity of identified pain-modulating neurons, the ON- and OFF-cells. Thus the present study fills an important gap, revealing a novel *functional* link between an

ascending nociceptive transmission pathway (PB) and the primary output node (RVM) of a descending pain-modulating circuit. Additional research will be needed to determine whether the influence of PB on RVM is mediated by direct connections, and how this circuit is modified in persistent pain states.

## Acknowledgments

Supported by grants from NIH (R01 NS066159, R56 NS093894). QC was supported by F31 NS087634

## References

1. Barbaro NM, Heinricher MM, Fields HL. Putative nociceptive modulatory neurons in the rostral ventromedial medulla of the rat display highly correlated firing patterns. *Somatosens Mot Res.* 1989; 6:413–425. [PubMed: 2547274]
2. Behbehani MM, Zemlan FP. Response of nucleus raphe magnus neurons to electrical stimulation of nucleus cuneiformis: Role of acetylcholine. *Brain Res.* 1986; 369:110–118. [PubMed: 3697735]
3. Beitz AJ. The nuclei of origin of brain stem enkephalin and substance p projections to the rodent nucleus raphe magnus. *Neuroscience.* 1982; 7:2753–2768. [PubMed: 6185878]
4. Bernard JF, Bandler R. Parallel circuits for emotional coping behaviour: New pieces in the puzzle. *J Comp Neurol.* 1998; 401:429–436. [PubMed: 9826271]
5. Bernard JF, Besson JM. The spino(trigemino)pontoamygdaloid pathway: Electrophysiological evidence for an involvement in pain processes. *J Neurophysiol.* 1990; 63:473–490. [PubMed: 2329357]
6. Bernard JF, Dallel R, Raboisson P, Villanueva L, Le Bars D. Organization of the efferent projections from the spinal cervical enlargement to the parabrachial area and periaqueductal gray: A PHA-L study in the rat. *J Comp Neurol.* 1995; 353:480–505. [PubMed: 7759612]
7. Bernard JF, Huang GF, Besson JM. The parabrachial area: Electrophysiological evidence for an involvement in visceral nociceptive processes. *J Neurophysiol.* 1994; 71:1646–1660. [PubMed: 8064340]
8. Bester H, Chapman V, Besson JM, Bernard JF. Physiological properties of the lamina i spinoparabrachial neurons in the rat. *J Neurophysiol.* 2000; 83:2239–2259. [PubMed: 10758132]
9. Bourgeois L, Monconduit L, Villanueva L, Bernard JF. Parabrachial internal lateral neurons convey nociceptive messages from the deep laminae of the dorsal horn to the intralaminar thalamus. *J Neurosci.* 2001; 21:2159–2165. [PubMed: 11245700]
10. Burgess SE, Gardell LR, Ossipov MH, Malan TP Jr, Vanderah TW, Lai J, Porreca F. Time-dependent descending facilitation from the rostral ventromedial medulla maintains, but does not initiate, neuropathic pain. *J Neurosci.* 2002; 22:5129–5136. [PubMed: 12077208]
11. Carlson JD, Maire JJ, Martenson ME, Heinricher MM. Sensitization of pain-modulating neurons in the rostral ventromedial medulla after peripheral nerve injury. *J Neurosci.* 2007; 27:13222–13231. [PubMed: 18045916]
12. Chamberlin NL, Saper CB. Topographic organization of cardiovascular responses to electrical and glutamate microstimulation of the parabrachial nucleus in the rat. *J Comp Neurol.* 1992; 326:245–262. [PubMed: 1362207]
13. Chamberlin NL, Saper CB. Topographic organization of respiratory responses to glutamate microstimulation of the parabrachial nucleus in the rat. *J Neurosci.* 1994; 14:6500–6510. [PubMed: 7965054]
14. Chen Z, Xie F, Bao M, Li X, Chao Y, Lin C, Guo R, Zhang C, Wu A, Yue Y, Guan Y, Wang Y. Activation of p38 MAPK in the rostral ventromedial medulla by visceral noxious inputs transmitted via the dorsal columns may contribute to pelvic organ cross-sensitization in rats with endometriosis. *Neuroscience.* 2015; 291:272–278. [PubMed: 25701711]
15. Cleary DR, Heinricher MM. Adaptations in responsiveness of brainstem pain-modulating neurons in acute compared with chronic inflammation. *Pain.* 2013; 154:845–855. [PubMed: 23588008]

16. Cleary DR, Phillips RS, Wallisch M, Heinricher MM. A novel, non-invasive method of respiratory monitoring for use with stereotactic procedures. *J Neurosci Meth.* 2012; 209:337–343.
17. Coizet V, Dommett EJ, Klop EM, Redgrave P, Overton PG. The parabrachial nucleus is a critical link in the transmission of short latency nociceptive information to midbrain dopaminergic neurons. *Neuroscience.* 2010; 168:263–272. [PubMed: 20363297]
18. D'Hanis W, Linke R, Yilmazer-Hanke DM. Topography of thalamic and parabrachial calcitonin gene-related peptide (CGRP) immunoreactive neurons projecting to subnuclei of the amygdala and extended amygdala. *J Comp Neurol.* 2007; 505:268–291. [PubMed: 17879271]
19. Davern PJ. A role for the lateral parabrachial nucleus in cardiovascular function and fluid homeostasis. *Front Physiol.* 2014; 5:436. [PubMed: 25477821]
20. De Felice M, Sanoja R, Wang R, Vera-Portocarrero L, Oyarzo J, King T, Ossipov MH, Vanderah TW, Lai J, Dussor GO, Fields HL, Price TJ, Porreca F. Engagement of descending inhibition from the rostral ventromedial medulla protects against chronic neuropathic pain. *Pain.* 2011; 152:2701–2709. [PubMed: 21745713]
21. Edelmayer RM, Vanderah TW, Majuta L, Zhang ET, Fioravanti B, De Felice M, Chichorro JG, Ossipov MH, King T, Lai J, Kori SH, Nelsen AC, Cannon KE, Heinricher MM, Porreca F. Medullary pain facilitating neurons mediate allodynia in headache-related pain. *Ann Neurol.* 2009; 65:184–193. [PubMed: 19259966]
22. Feil K, Herbert H. Topographic organization of spinal and trigeminal somatosensory pathways to the rat parabrachial and Kölliker-Fuse nuclei. *J Comp Neurol.* 1995; 353:506–528. [PubMed: 7759613]
23. Fields HL, Heinricher MM. Anatomy and physiology of a nociceptive modulatory system. *Philos Trans of the R Soc Lond B Biol Sci.* 1985; 308:361–374.
24. Fuller PM, Sherman D, Pedersen NP, Saper CB, Lu J. Reassessment of the structural basis of the ascending arousal system. *J Comp Neurol.* 2011; 519:933–956. [PubMed: 21280045]
25. Fulwiler CE, Saper CB. Subnuclear organization of the efferent connections of the parabrachial nucleus in the rat. *Brain Res.* 1984; 319:229–259. [PubMed: 6478256]
26. Gauriau C, Bernard JF. Pain pathways and parabrachial circuits in the rat. *Exp Physiol.* 2002; 87:251–258. [PubMed: 11856971]
27. Han JS, Adwanikar H, Li Z, Ji G, Neugebauer V. Facilitation of synaptic transmission and pain responses by CGRP in the amygdala of normal rats. *Mol Pain.* 2010; 6:10. [PubMed: 20144185]
28. Han S, Soleiman MT, Soden ME, Zweifel LS, Palmiter RD. Elucidating an affective pain circuit that creates a threat memory. *Cell.* 2015; 162:363–374. [PubMed: 26186190]
29. Heinricher MM, Barbaro NM, Fields HL. Putative nociceptive modulating neurons in the rostral ventromedial medulla of the rat: Firing of on- and off-cells is related to nociceptive responsiveness. *Somatosens Mot Res.* 1989; 6:427–439. [PubMed: 2547275]
30. Heinricher MM, Drasner K. Lumbar intrathecal morphine alters activity of putative nociceptive modulatory neurons in rostral ventromedial medulla. *Brain Res.* 1991; 549:338–341. [PubMed: 1884228]
31. Heinricher, MM.; Fields, HL. Central nervous system mechanisms of pain modulation. In: McMahon, S.; Koltzenburg, M.; Tracey, I.; Turk, DC., editors. *Wall and Melzack's textbook of pain.* 6th. London: Elsevier; 2013. p. 129-142.
32. Heinricher, MM.; Ingram, SL. The brainstem and nociceptive modulation. In: Bushnell, MC.; Basbaum, AI., editors. *The science of pain.* San Diego: Academic Press; 2008. p. 593-626.
33. Heinricher MM, Kaplan HJ. GABA-mediated inhibition in rostral ventromedial medulla: Role in nociceptive modulation in the lightly anesthetized rat. *Pain.* 1991; 47:105–113. [PubMed: 1663224]
34. Heinricher MM, Neubert MJ, Martenson ME, Gonçalves L. Prostaglandin E<sub>2</sub> in the medial preoptic area produces hyperalgesia and activates pain-modulating circuitry in the rostral ventromedial medulla. *Neuroscience.* 2004; 128:389–398. [PubMed: 15350650]
35. Heinricher MM, Tavares I, Leith JL, Lumb BM. Descending control of nociception: Specificity, recruitment and plasticity. *Brain Res Rev.* 2009; 60:214–225. [PubMed: 19146877]
36. Hermann DM, Luppi PH, Peyron C, Hinckel P, Jouvet M. Afferent projections to the rat nuclei raphe magnus, raphe pallidus and reticularis gigantocellularis pars alpha demonstrated by

- iontophoretic application of cholera toxin (subunit b). *J Chem Neuroanat.* 1997; 13:1–21. [PubMed: 9271192]
37. Hermanson O, Blomqvist A. Subnuclear localization of FOS-like immunoreactivity in the rat parabrachial nucleus after nociceptive stimulation. *J Comp Neurol.* 1996; 368:45–56. [PubMed: 8725293]
  38. Hernandez N, Lopez Y, Vanegas H. Medullary on- and off-cell responses precede both segmental and thalamic responses to tail heating. *Pain.* 1989; 39:221–230. [PubMed: 2594400]
  39. Horiuchi J, McAllen RM, Allen AM, Killinger S, Fontes MA, Dampney RA. Descending vasomotor pathways from the dorsomedial hypothalamic nucleus: Role of medullary raphe and RVLM. *Am J Physiol Regul Integr Comp Physiol.* 2004; 287:R824–R832. [PubMed: 15205184]
  40. Jasmin L, Burkey AR, Card JP, Basbaum AI. Transneuronal labeling of a nociceptive pathway, the spino-(trigemino-)parabrachio-amygdaloid, in the rat. *J Neurosci.* 1997; 17:3751–3765. [PubMed: 9133395]
  41. Jasmin L, Rabkin SD, Granato A, Boudah A, Ohara PT. Analgesia and hyperalgesia from GABA-mediated modulation of the cerebral cortex. *Nature.* 2003; 424:316–320. [PubMed: 12867983]
  42. Jinks SL, Carstens EE, Antognini JF. Glutamate receptor blockade in the rostral ventromedial medulla reduces the force of multisegmental motor responses to supramaximal noxious stimuli. *Neurosci Lett.* 2007; 426:175–180. [PubMed: 17904740]
  43. Kaur S, Pedersen NP, Yokota S, Hur EE, Fuller PM, Lazarus M, Chamberlin NL, Saper CB. Glutamatergic signaling from the parabrachial nucleus plays a critical role in hypercapnic arousal. *J Neurosci.* 2013; 33:7627–7640. [PubMed: 23637157]
  44. Khasabov SG, Ghilardi JR, Mantyh PW, Simone DA. Spinal neurons that express NK-1 receptors modulate descending controls that project through the dorsolateral funiculus. *J Neurophysiol.* 2005; 93:998–1006. [PubMed: 15456795]
  45. Kincaid W, Neubert MJ, Xu M, Kim CJ, Heinricher MM. Role for medullary pain facilitating neurons in secondary thermal hyperalgesia. *J Neurophysiol.* 2006; 95:33–41. [PubMed: 16192337]
  46. Kruger L, Sternini C, Brecha NC, Mantyh PW. Distribution of calcitonin gene-related peptide immunoreactivity in relation to the rat central somatosensory projection. *J Comp Neurol.* 1988; 273:149–162. [PubMed: 3047185]
  47. Lapirot O, Chebbi R, Monconduit L, Artola A, Dallel R, Luccarini P. Nk1 receptor-expressing spinoparabrachial neurons trigger diffuse noxious inhibitory controls through lateral parabrachial activation in the male rat. *Pain.* 2009; 142:245–254. [PubMed: 19231081]
  48. Lewis GN, Rice DA, McNair PJ. Conditioned pain modulation in populations with chronic pain: A systematic review and meta-analysis. *J Pain.* 2012; 13:936–944. [PubMed: 22981090]
  49. Martenson ME, Cetas JS, Heinricher MM. A possible neural basis for stress-induced hyperalgesia. *Pain.* 2009; 142:236–244. [PubMed: 19232470]
  50. Martenson ME, Halawa OI, Tonsfeldt KJ, Maxwell CA, Hammack N, Mist SD, Pennesi ME, Bennett RM, Mauer KM, Jones KD, Heinricher MM. A possible neural mechanism for photosensitivity in chronic pain. *Pain.* 2016; 157:868–878. [PubMed: 26785323]
  51. McGaraughty S, Farr DA, Heinricher MM. Lesions of the periaqueductal gray disrupt input to the rostral ventromedial medulla following microinjections of morphine into the medial or basolateral nuclei of the amygdala. *Brain Res.* 2004; 1009:223–227. [PubMed: 15120601]
  52. McGaraughty S, Heinricher MM. Microinjection of morphine into various amygdaloid nuclei differentially affects nociceptive responsiveness and rvm neuronal activity. *Pain.* 2002; 96:153–162. [PubMed: 11932071]
  53. Morrison SF. Central neural pathways for thermoregulatory cold defense. *J Appl Physiol* (1985). 2011; 110:1137–1149. [PubMed: 21270352]
  54. Morrison SF, Madden CJ, Tupone D. Central control of brown adipose tissue thermogenesis. *Front Endocrinol (Lausanne).* 2012;3. [PubMed: 22649403]
  55. Nakamura K, Morrison SF. Central efferent pathways for cold-defensive and febrile shivering. *J Physiol.* 2011; 589:3641–3658. [PubMed: 21610139]

56. Nichols ML, Allen BJ, Rogers SD, Ghilardi JR, Honore P, Luger NM, Finke MP, Li J, Lappi DA, Simone DA, Mantyh PW. Transmission of chronic nociception by spinal neurons expressing the substance p receptor. *Science*. 1999; 286:1558–1561. [PubMed: 10567262]
57. Paxinos, G.; Watson, C. *The rat brain in stereotaxic coordinates, compact*. 6th. Amsterdam: Academic Press; 2009.
58. Polgár E, Wright LL, Todd AJ. A quantitative study of brainstem projections from lamina I neurons in the cervical and lumbar enlargement of the rat. *Brain Res*. 2010; 1308:58–67. [PubMed: 19854164]
59. Porreca F, Burgess SE, Gardell LR, Vanderah TW, Malan TP Jr, Ossipov MH, Lappi DA, Lai J. Inhibition of neuropathic pain by selective ablation of brainstem medullary cells expressing the  $\mu$ -opioid receptor. *J Neurosci*. 2001; 21:5281–5288. [PubMed: 11438603]
60. Porreca F, Ossipov MH, Gebhart GF. Chronic pain and medullary descending facilitation. *Trends Neurosci*. 2002; 25:319–325. [PubMed: 12086751]
61. Ren K, Dubner R. Descending modulation in persistent pain: An update. *Pain*. 2002; 100:1–6. [PubMed: 12435453]
62. Rivat C, Vera-Portocarrero LP, Ibrahim MM, Mata HP, Stagg NJ, De Felice M, Porreca F, Malan TP. Spinal NK-1 receptor-expressing neurons and descending pathways support fentanyl-induced pain hypersensitivity in a rat model of postoperative pain. *Eur J Neurosci*. 2009; 29:727–737. [PubMed: 19200067]
63. Samuels BC, Zaretsky DV, DiMicco JA. Tachycardia evoked by disinhibition of the dorsomedial hypothalamus in rats is mediated through medullary raphe. *J Physiol*. 2002; 538:941–946. [PubMed: 11826177]
64. Samuels BC, Zaretsky DV, DiMicco JA. Dorsomedial hypothalamic sites where disinhibition evokes tachycardia correlate with location of raphe-projecting neurons. *Am J Physiol Regul Integr Comp Physiol*. 2004; 287:R472–R478. [PubMed: 15072966]
65. Sato F, Akhter F, Haque T, Kato T, Takeda R, Nagase Y, Sessle BJ, Yoshida A. Projections from the insular cortex to pain-receptive trigeminal caudal subnucleus (medullary dorsal horn) and other lower brainstem areas in rats. *Neuroscience*. 2013; 233:9–27. [PubMed: 23270856]
66. Schwaber JS, Sternini C, Brecha NC, Rogers WT, Card JP. Neurons containing calcitonin gene-related peptide in the parabrachial nucleus project to the central nucleus of the amygdala. *J Comp Neurol*. 1988; 270:416–426. 398-419. [PubMed: 2836477]
67. Sugiyo S, Takemura M, Dubner R, Ren K. Trigeminal transition zone/rostral ventromedial medulla connections and facilitation of orofacial hyperalgesia after masseter inflammation in rats. *J Comp Neurol*. 2005; 493:510–523. [PubMed: 16304628]
68. Suzuki R, Morcuende S, Webber M, Hunt SP, Dickenson AH. Superficial NK1-expressing neurons control spinal excitability through activation of descending pathways. *Nat Neurosci*. 2002; 5:1319–1326. [PubMed: 12402039]
69. Suzuki R, Rygh LJ, Dickenson AH. Bad news from the brain: Descending 5-HT pathways that control spinal pain processing. *Trends Pharmacol Sci*. 2004; 25:613–617. [PubMed: 15530638]
70. Tomim DH, Pontarolla FM, Bertolini JF, Arase M, Tobaldini G, Lima MM, Fischer L. The pronociceptive effect of paradoxical sleep deprivation in rats: Evidence for a role of descending pain modulation mechanisms. *Mol Neurobiol*. 2015
71. Urban MO, Gebhart GF. Supraspinal contributions to hyperalgesia. *Proc Natl Acad Sci U S A*. 1999; 96:7687–7692. [PubMed: 10393881]
72. Vanegas H, Schaible H-G. Descending control of persistent pain: Inhibitory or facilitatory? *Brain Res Rev*. 2004; 46:295–309. [PubMed: 15571771]
73. Vera-Portocarrero LP, Xie JY, Kowal J, Ossipov MH, King T, Porreca F. Descending facilitation from the rostral ventromedial medulla maintains visceral pain in rats with experimental pancreatitis. *Gastroenterology*. 2006; 130:2155–2164. [PubMed: 16762636]
74. Vera-Portocarrero LP, Zhang ET, King T, Ossipov MH, Vanderah TW, Lai J, Porreca F. Spinal NK-1 receptor expressing neurons mediate opioid-induced hyperalgesia and antinociceptive tolerance via activation of descending pathways. *Pain*. 2007; 129:35–45. [PubMed: 17123731]
75. Verner TA, Pilowsky PM, Goodchild AK. Retrograde projections to a discrete apneic site in the midline medulla oblongata of the rat. *Brain Res*. 2008; 1208:128–136. [PubMed: 18387596]



76. Xu M, Kim CJ, Neubert MJ, Heinricher MM. Nmda receptor-mediated activation of medullary pro-nociceptive neurons is required for secondary thermal hyperalgesia. *Pain*. 2007; 127:253–262. [PubMed: 16997469]
77. Yarnitsky D. Conditioned pain modulation (the diffuse noxious inhibitory control-like effect): Its relevance for acute and chronic pain states. *Curr Opin Anaesthesiol*. 2010; 23:611–615. [PubMed: 20543676]
78. Yasui Y, Saper CB, Cechetto DF. Calcitonin gene-related peptide immunoreactivity in the visceral sensory cortex, thalamus, and related pathways in the rat. *J Comp Neurol*. 1989; 290:487–501. [PubMed: 2613940]
79. Zemlan FP, Behbehani MM. Nucleus cuneiformis and pain modulation: Anatomy and behavioral pharmacology. *Brain Res*. 1988; 453:89–102. [PubMed: 2456838]

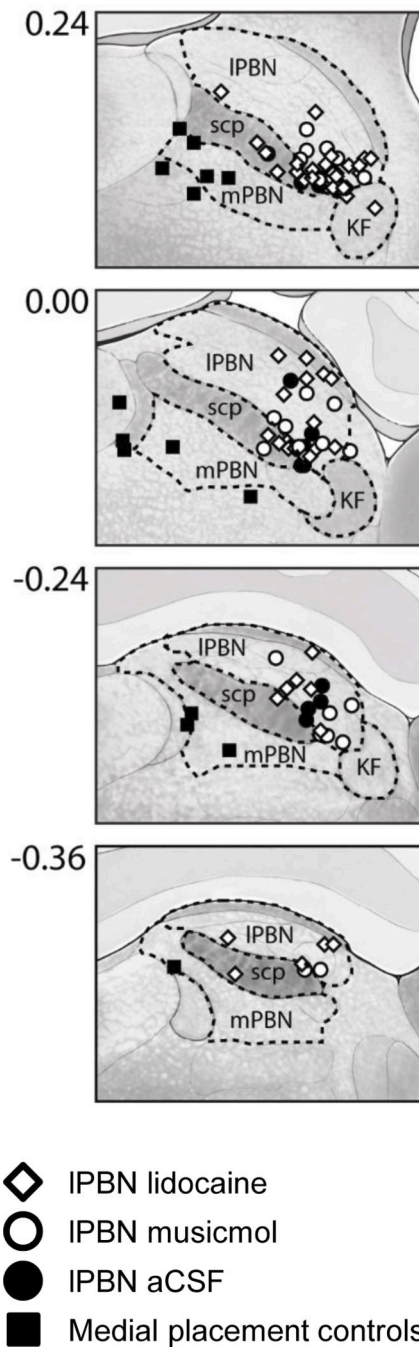


**Fig. 1.** Locations of microinjection sites in the lateral PB complex and medial PB area. Injections were distributed among sections at +0.24 to -0.36 relative to the interaural line. KF: Kölliker-Fuse, IPB: lateral parabrachial complex, mPB: medial parabrachial area, scp: superior cerebellar peduncle.

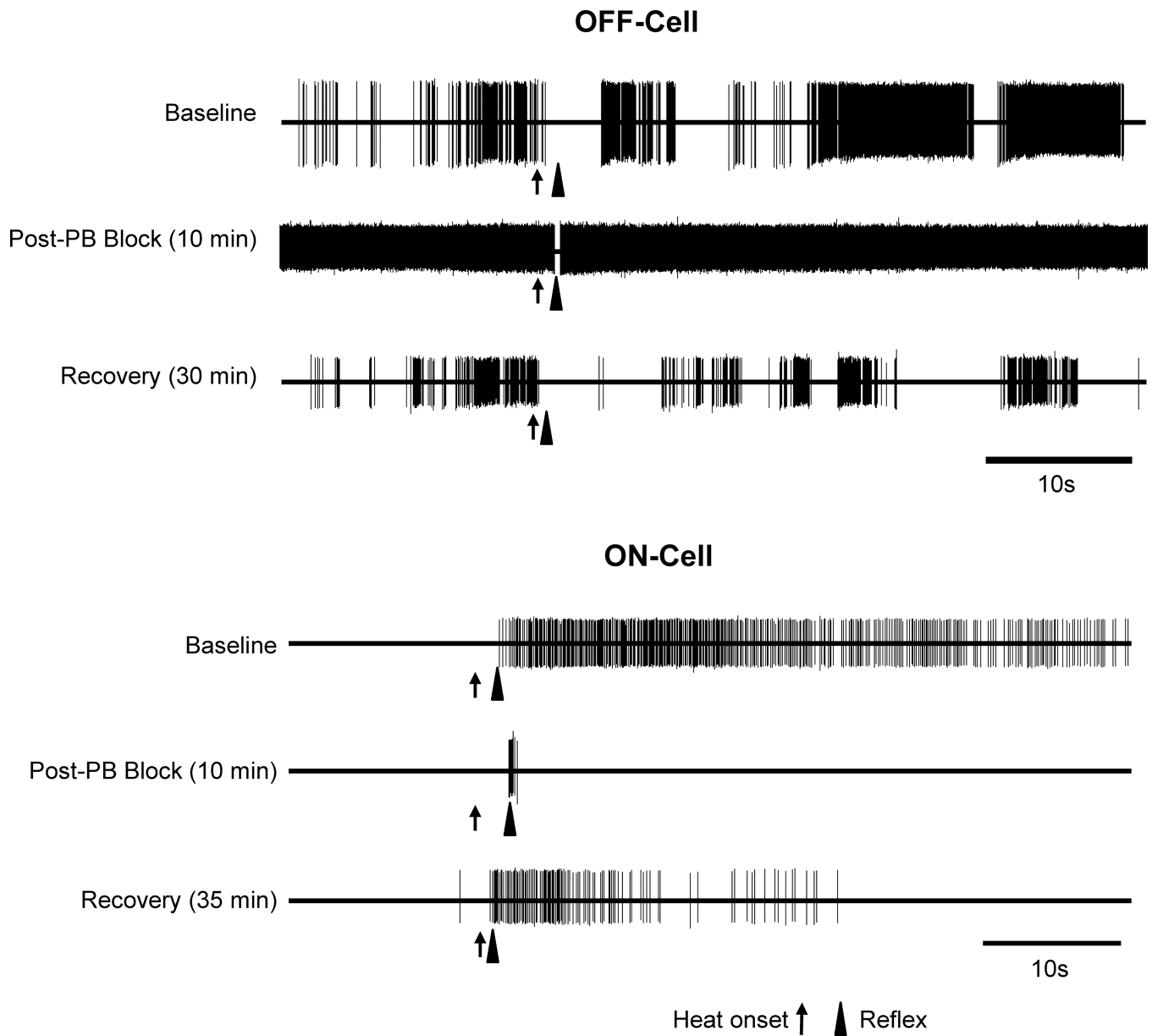


**Fig. 2. Examples of the effect of lateral PB block on noxious stimulus-evoked, reflex-related activity of ON- and OFF-cells**  
 Representative examples show OFF- and ON-cell activity during withdrawal from noxious heat stimulus at baseline compared to during lidocaine block of lateral PB contralateral to the stimulus, as well as subsequent recovery. In both cases, reflex-related changes in firing were substantially reduced, although not entirely eliminated. Increased spontaneous firing of the OFF-cell is also evident.

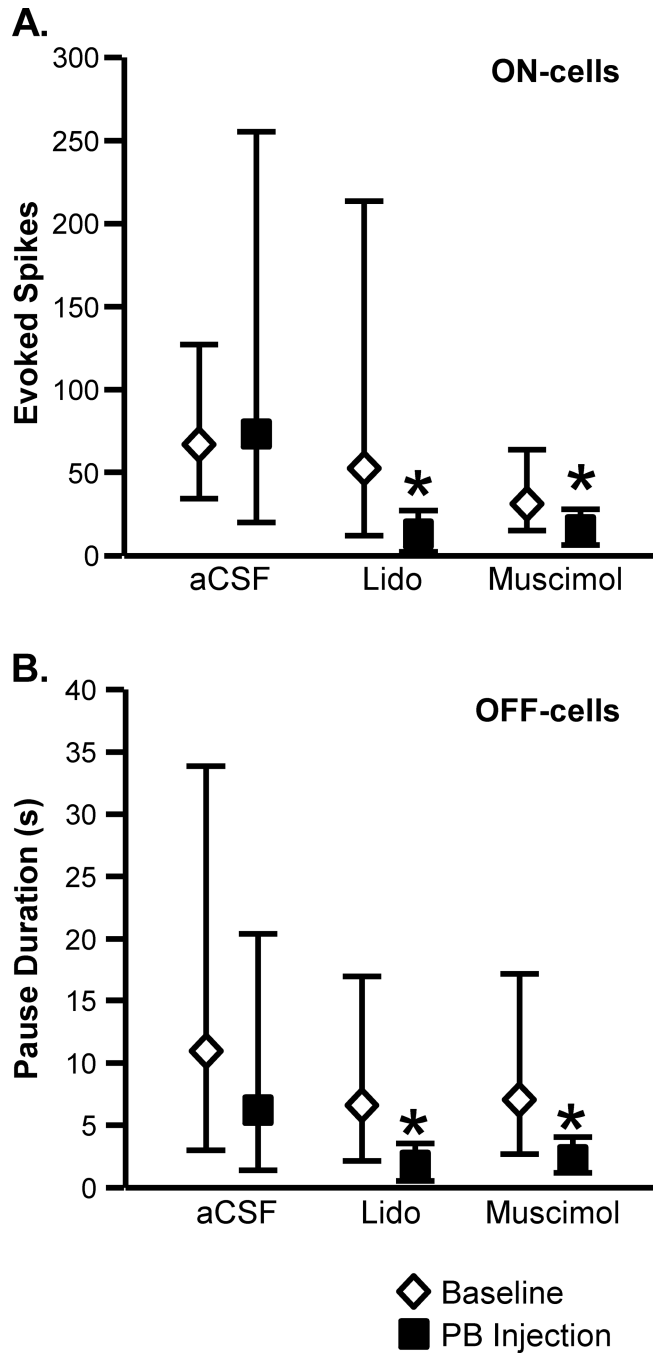


**Fig. 3. Inactivation of lateral PB interfered with the ON-cell burst and OFF-cell pause in response to heat stimulation**  
**A.** ON-cells. Effect of lateral PB microinjection of aCSF (200 nl), lidocaine (4%, 200 nl), or muscimol (8 pmol in 200 nl) on the ON-cell burst (measured as total evoked spikes). **B.** OFF-cells. Effect of lateral PB microinjection of aCSF, lidocaine, or muscimol on OFF-cell pause (measured as pause duration). (PB injections were contralateral to the peripheral stimulus. Reported as geometric mean with 95% confidence limits, \* $p < 0.05$  compared to baseline,  $t$ -test for correlated means,  $n = 8$  to 11 cells per class/treatment.)

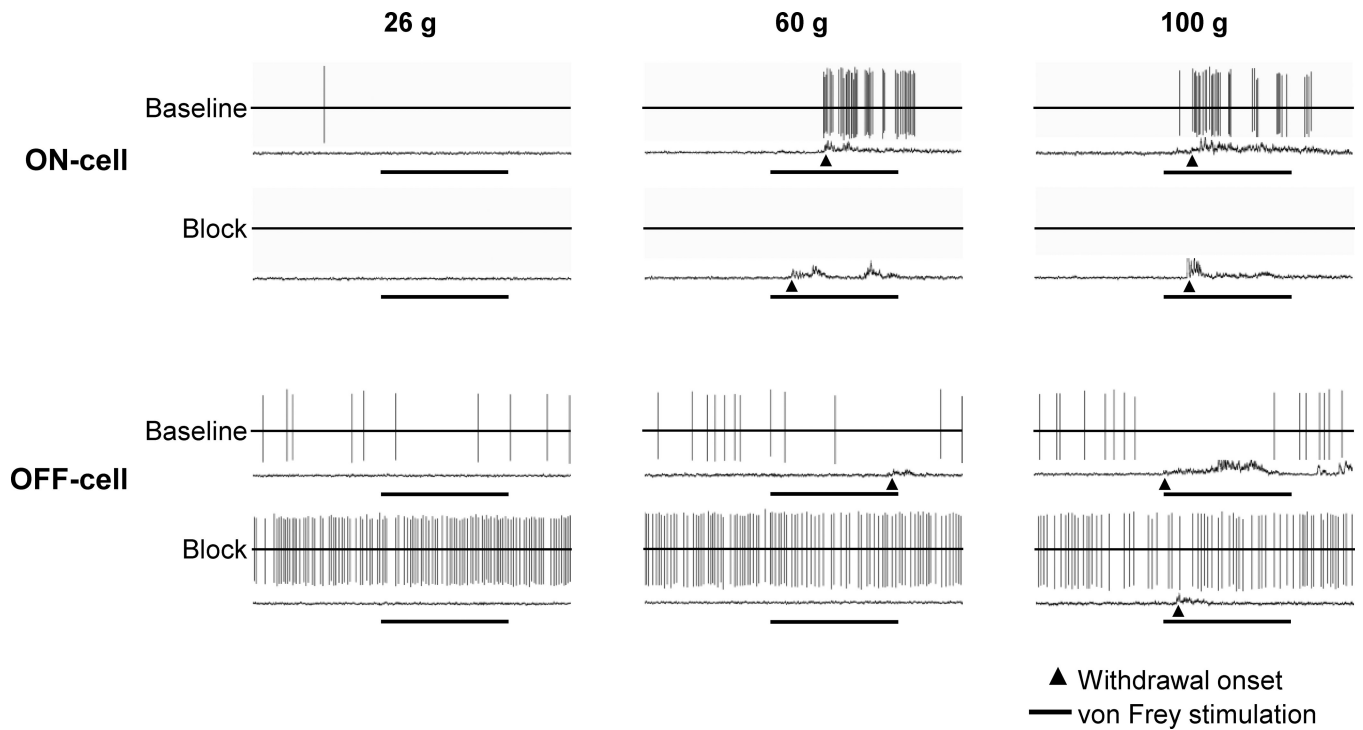


**Fig. 4. Examples of the effect of lateral PB block on mechanically evoked, reflex-related activity of ON- and OFF-cells**

Representative examples show ON- and OFF-cell activity and associated EMG during trials using 26, 60, and 100 g von Frey probes both in baseline and during PB block. A baseline (top-trace) and block trial (lower trace) are shown for each force. Reflex-related changes in firing were substantially reduced in both cases, and even eliminated for the ON-cell. Period of von Frey fiber application (8 s) is shown below each trace, with arrowhead indicating behavioral responses, which occurred in response to 60 and 100 g stimuli in baseline.

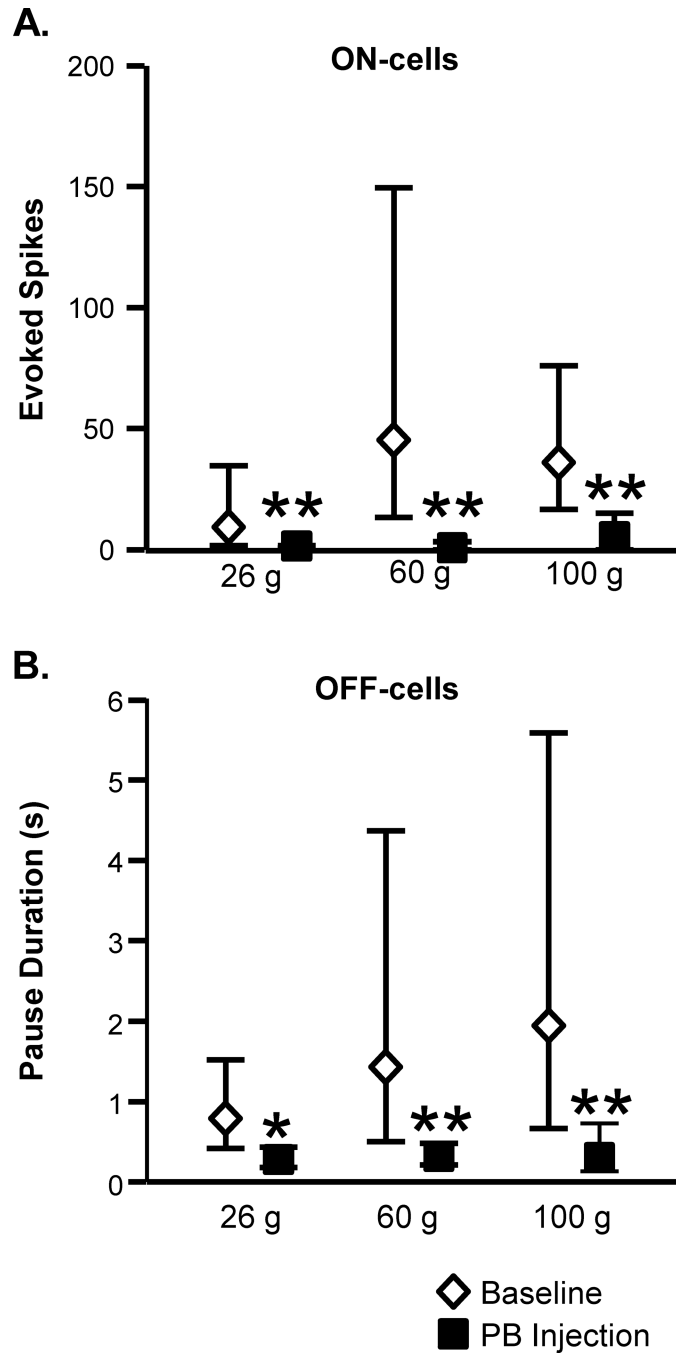


**Fig. 5. Inactivation of lateral PB interfered with the ON-cell burst and OFF-cell pause in response to mechanical stimulation**

**A.** ON-cells. Effect of lidocaine (4%, 200 nl) microinjected into the lateral PB on activity triggered during application of von Frey probes (26, 60 and 100 g, measured as total evoked spikes,  $n = 8$ ). **B.** OFF-cells. Effect of lidocaine (4%, 200 nl) microinjected into the lateral PB on OFF-cell pause (measured as pause duration,  $n = 13$ ). (PB injections were contralateral to the peripheral stimulus. Reported as geometric mean with 95% confidence limits,  $t$ -test for correlated means,  $*p < 0.05$ ,  $**p < 0.01$  compared to baseline.)

## Statistical analysis.

ON-cells (n = 8): 26 g:  $t_7 = 3.80$ ,  $p = 0.0067$ ; 60 g:  $t_5 = 6.99$ ,  $p = 0.0009$  (two cells active at stimulus onset; 100 g:  $t_7 = 3.77$ ,  $p = 0.0069$ ).

OFF-cells (n = 13): 26 g:  $t_{11} = 2.67$ ,  $p = 0.022$  (one cell silent at stimulus onset); 60 g:  $t_{11} = 3.17$ ,  $p = 0.009$  (one cell silent at stimulus onset); 100 g:  $t_{11} = 3.81$ ,  $p = 0.0029$  (one cell silent at stimulus onset).

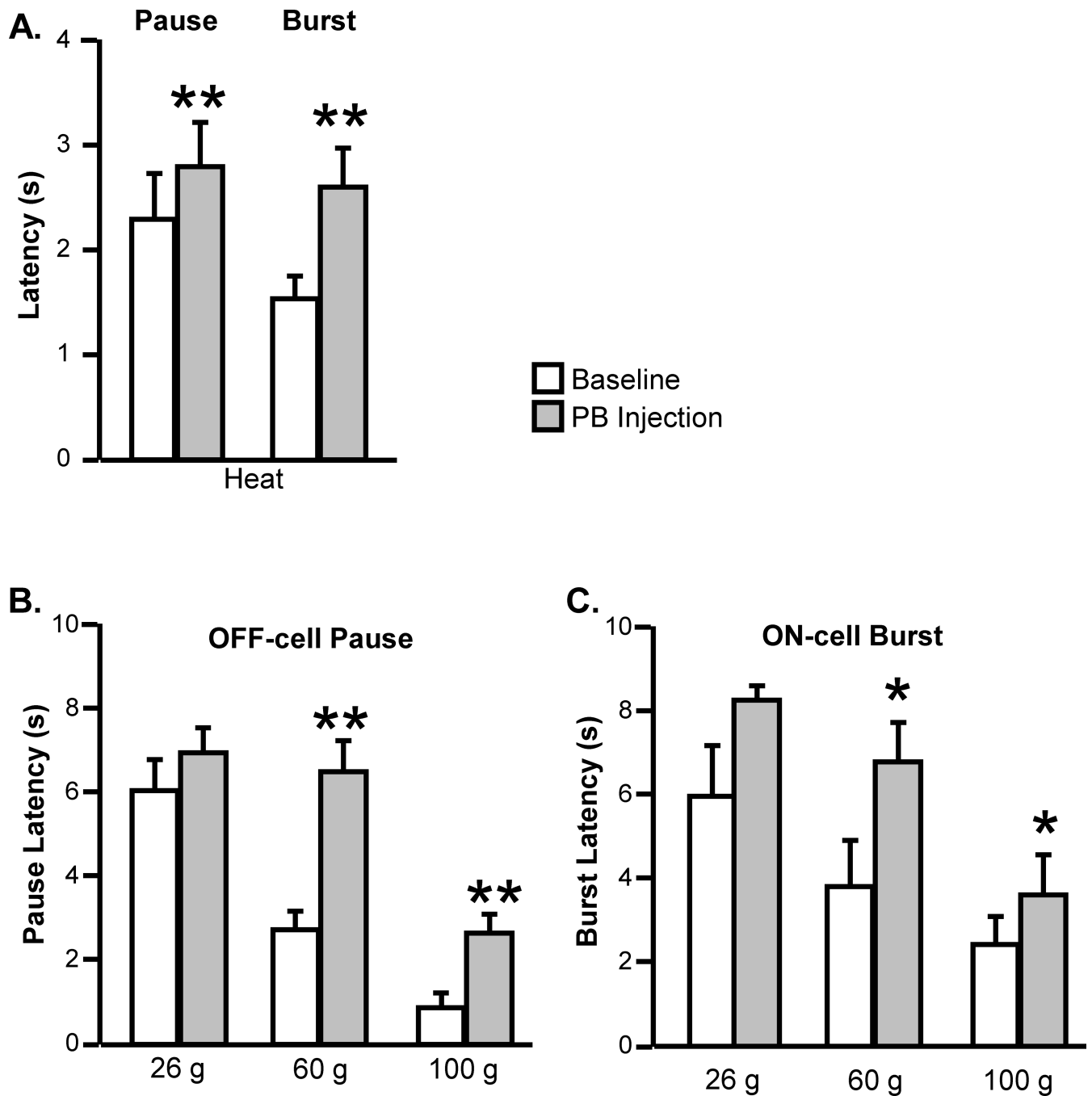


**Fig. 6. The latencies of the residual ON-cell burst and OFF-cell pause were increased during inactivation of lateral PB**

Effect of lateral PB block (lidocaine) on the latencies of the ON-cell burst and OFF-cell pause during noxious heat (A) and stimulation with VF probes (26, 60 and 100 g, B and C). (PB injections were contralateral to the peripheral stimulus. Mean + SEM, \* $p < 0.05$ , \*\* $p < 0.01$  compared to baseline using  $t$ -test for correlated means or Wilcoxon's signed ranks test, 8 to 13 cells/group)

Statistical analysis:



Heat. Pause:  $t_{10} = 3.93$ ,  $p = 0.0028$ ,  $n = 11$ , Burst:  $t_{10} = 3.84$ ,  $p = 0.0033$ ,  $n = 11$ .

Mechanical stimulation, pause. 26 g:  $W = 11$ ,  $p = 0.19$ ,  $n = 13$ ; 60 g:  $W = 78$ ,  $p = 0.0005$ ,  $n = 13$  (with one cell silent); 100 g:  $W = 74$ ,  $p = 0.0015$ ,  $n = 13$  (with one cell silent).

Mechanical stimulation, burst. 26 g:  $W = 10$ ,  $p = 0.12$ ,  $n = 8$ ; 60 g:  $W = 21$ ,  $p = 0.031$ ,  $n = 8$  (two cells active); 100 g:  $W = 24$ ,  $p = 0.047$ ,  $n = 8$ .

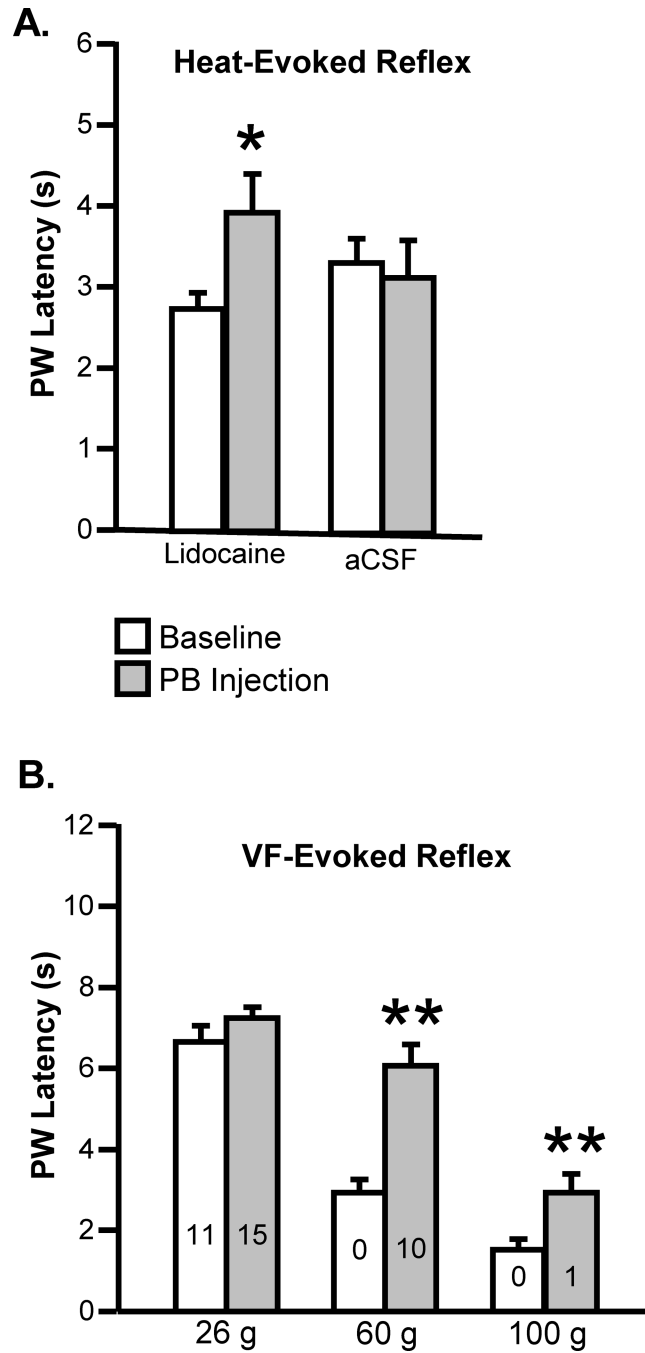


**Fig. 7. Modest behavioral hypoalgesia during inactivation of lateral PB**  
**A.** Effect of lidocaine or aCSF microinjected into the lateral PB on latency to heat-evoked withdrawal. Latency was significantly increased during lidocaine block of PB ( $t_{25} = 2.17$ ,  $p = 0.040$ ,  $n = 26$ ), but unaffected by injection of aCSF ( $t_{14} = 0.43$ ,  $p = 0.68$ ,  $n = 15$ ). **B.** Effect of lidocaine microinjected into the lateral PB on withdrawal evoked by VF probes (26, 60 and 100 g,  $n = 22$ , number of animals not responding within 8 s cut-off time shown within each bar). Latency was increased for stimuli in the noxious range (60 g:  $W = 243$ ,  $p < 0.0001$ ,  $n = 22$ ; 100 g:  $W = 203$ ,  $p = 0.0004$ ,  $n = 22$ ) but not for the 26 g stimulus ( $W = 31$ ,  $p$

= 0.13, n = 22). PB injections were contralateral to the peripheral stimulus. (Data shown as mean + SEM, \* $p < 0.05$ , \*\* $p < 0.01$  compared to baseline using  $t$ -test for correlated means or Wilcoxon's signed ranks test.)

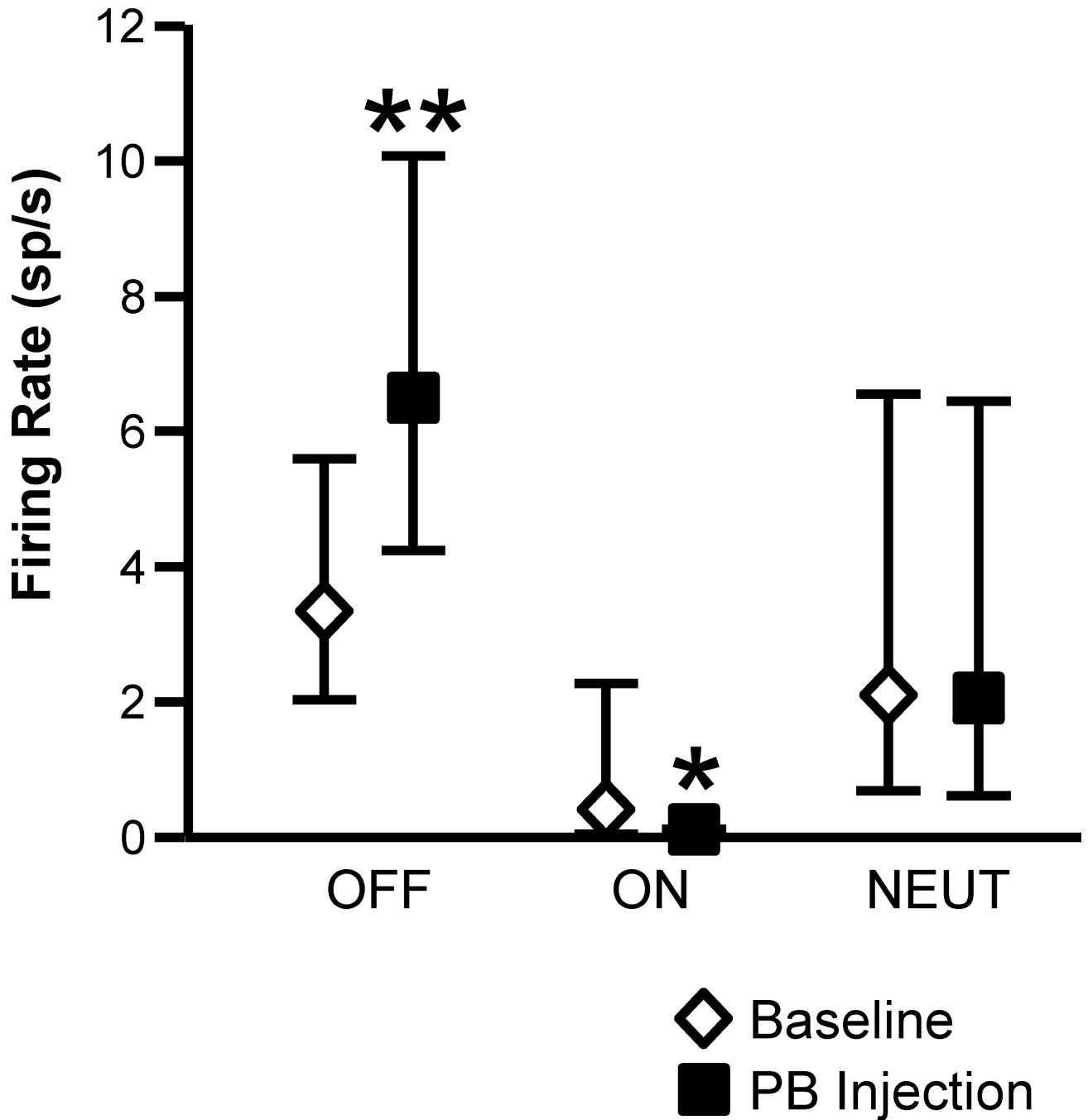


**Fig. 8. Effect of lidocaine (4%, 200 nl) microinjected into the lateral PB on spontaneous firing of OFF-cells, ON-cells, and NEUTRAL-cells in RVM**

OFF-cell firing was significantly increased ( $t_{12} = 3.77$ ,  $p = 0.0027$ ,  $n = 13$ ), while ON-cell firing was reduced ( $t_7 = 3.03$ ,  $p = 0.0019$ ,  $n = 8$ ). NEUTRAL-cells did not respond to lateral PB block ( $t_5 = 0.98$ ,  $p = 0.37$ ,  $n = 6$ ). (PB injection was unilateral. Geometric mean with 95% confidence limits, \* $p < 0.05$ , \*\* $p < 0.01$  compared to pre-block baseline using  $t$ -test for correlated means)

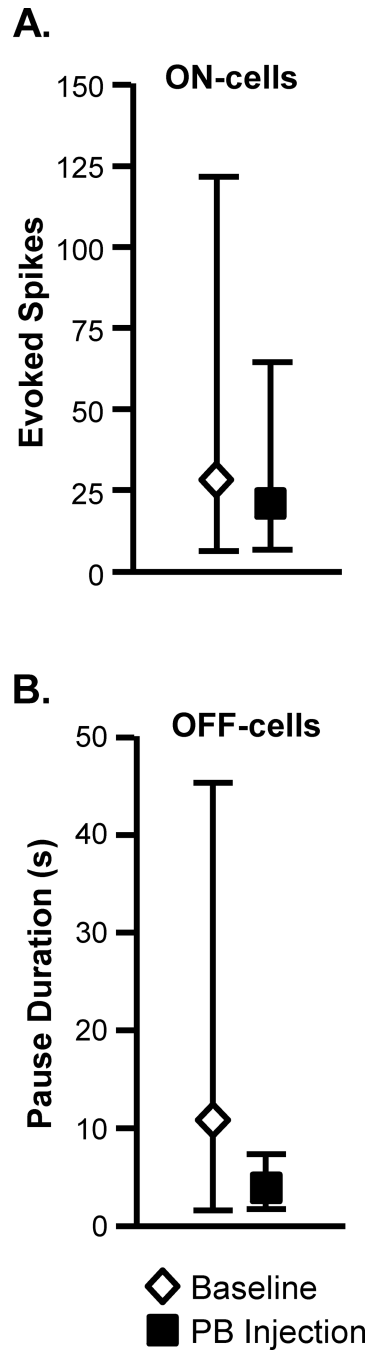


**Fig. 9. Medial PB (mPB) does not contribute to the ON-cell burst and OFF-cell pause**  
**A.** Muscimol (8 pmol in 200 nl) microinjected into the mPB and adjacent tegmentum had no effect on heat-evoked activity of ON-cells ( $t_7 = 1.26$ ,  $p = 0.25$ ,  $n = 8$ ). **B.** Muscimol (8 pmol in 200 nl) microinjected into the mPB and adjacent tegmentum had no effect on the heat-related OFF-cell pause ( $t_5 = 1.34$ ,  $p = 0.24$ ,  $n = 7$  with one neuron silent at heat onset). (PB injections were contralateral to the peripheral stimulus. Reported as geometric mean with 95% confidence limits.)

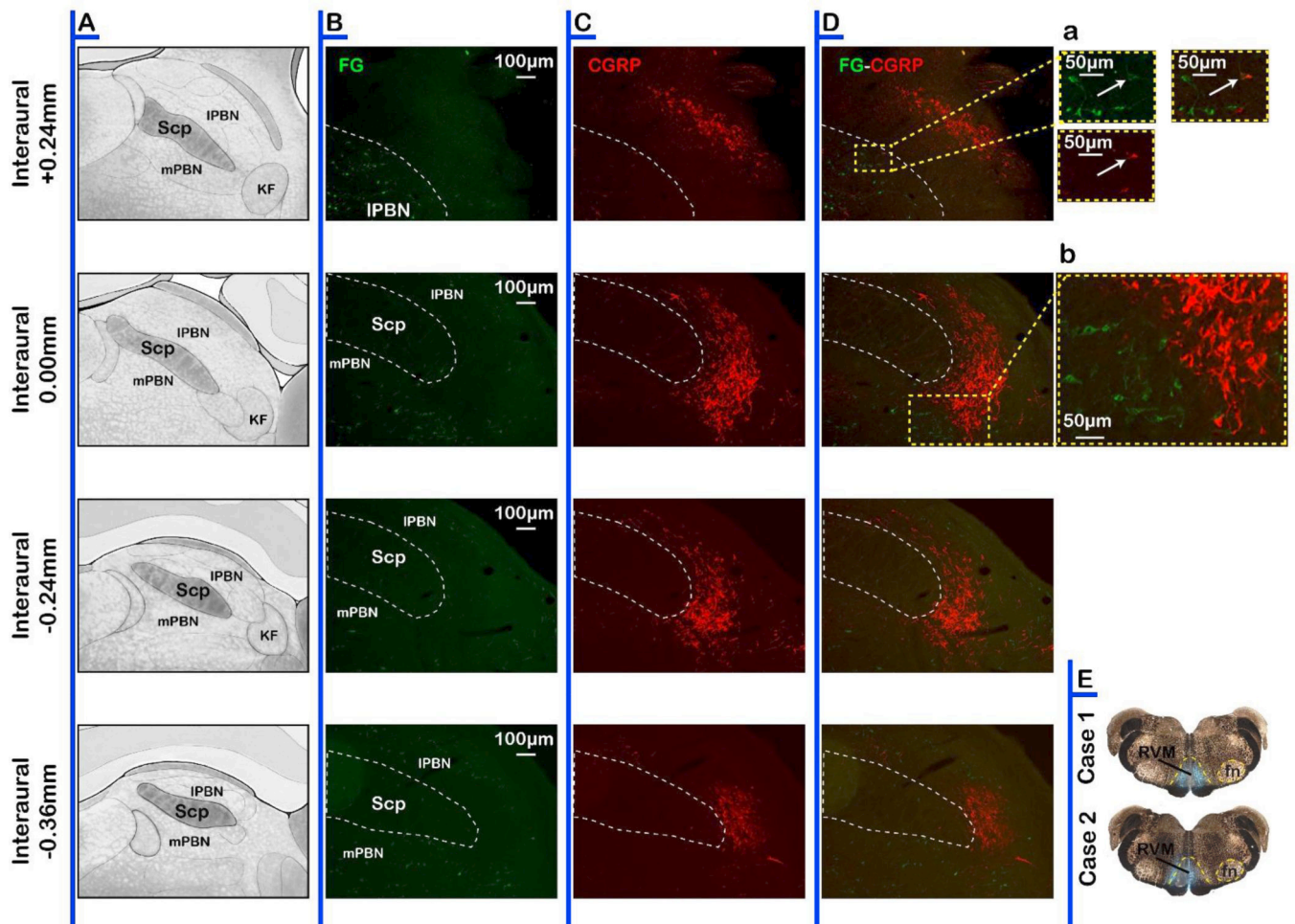


**Fig. 10. CGRP-ir neurons in PB do not project to the RVM**

**A** Schematic representation of the PB. Immunohistochemical label for FG (**B**, green), CGRP (**C**, red) and overlap (**D**) in the PB. **Da**. Inset showing higher magnification view of the only CGRP/FG double labeled neuron found in PB. **Db**. Inset showing higher magnification view illustrates segregation of CGRP-ir neurons from RVM-projecting neurons.